



# Synoptic and regional-scale meteorological controls of stratus altitude in the Namib Desert

Viola Hippler<sup>1</sup>, Hendrik Andersen<sup>1,2</sup>, Robert Spirig<sup>3</sup>, Roland Vogt<sup>3</sup>, Stuart Piketh<sup>4</sup>, Bianca Adler<sup>5,6</sup>, and Jan Cermak<sup>1,2</sup>

<sup>1</sup>Institute of Meteorology and Climate Research, Atmospheric Trace Gases and Remote Sensing, Karlsruhe Institute of Technology (KIT), Karlsruhe, Germany

<sup>2</sup>Institute of Photogrammetry and Remote Sensing, Karlsruhe Institute of Technology (KIT), Karlsruhe, Germany

<sup>3</sup>Department of Environmental Sciences, University of Basel, Basel, Switzerland

<sup>4</sup>North-West University, School for Geo- and Spatial Sciences, Potchefstroom, South Africa

<sup>5</sup>Cooperative Institute for Research in Environmental Sciences (CIRES), University of Colorado Boulder, Boulder, Colorado, USA

<sup>6</sup>NOAA Physical Sciences Laboratory, Boulder, Colorado, USA

**Correspondence:** Hendrik Andersen (hendrik.andersen@kit.edu)

**Abstract.** In the Namib Desert, fog is an essential water source and occurs when and where advected marine stratus clouds intersect with the land surface. However, the meteorological controls of the cloud base height are still insufficiently understood. This study aims to develop a basic understanding of the relevant processes. We combine satellite and in situ observations with large-scale meteorological data from reanalysis data (ERA5) to compare fog events to lifted stratus at the coast (low-cloud events). In fog situations, the marine boundary layer is shallower along the entire coastline than in low-cloud situations. This is found to be related to the large-scale high-pressure systems. Fog situations exhibit a weaker Atlantic High but elevated continental pressure. The weaker Atlantic High is connected to less pronounced near-surface winds along the coastline, less cold advection, and heat fluxes upstream of the study region, leading to the shallower marine boundary layer. Increased continental pressure facilitates the development of regional mountain-plain winds that may reduce the height of the coastal inversion. These mechanisms are highlighted in a case study of an off-season fog event. To assess the predictive power of the two high-pressure systems and the regional pressure pattern, a logistic regression is trained with three corresponding features. The classification outperformed a climatological baseline by  $\approx 10\%$ , suggesting that the features contain relevant process information. The results improve our understanding of the processes that determine the seasonal and day-to-day variability of fog versus elevated low-cloud occurrence in the Namib.

## 15 1 Introduction

In the hyperarid Namib Desert, fog is a frequently available water source for ecosystems and is therefore of great ecological importance. While fog water has been documented to be essential for animal (Seely, 1979) and plant species (Burke, 2007; Loots et al., 2019) as well as microbial communities (Ramond et al., 2019; Warren-Rhodes et al., 2013), fog can also act as a vector for nutrients and pollutants (Weathers et al., 2020), impacting biochemistry in the receiving regions (Warren-Rhodes



20 et al., 2013; Gottlieb et al., 2019). The frequency of fog events also determines the amount of harvestable water for human use (Shanyengana et al., 2002; Mupambwa et al., 2019). Climate models project southern Africa to become warmer and drier (Maúre et al., 2018), potentially reducing the positive impact fog can have in this unique ecosystem (Haensler et al., 2011). Therefore, a thorough understanding of the controlling factors of fog occurrence patterns is essential and needed to assess the future of the Namib Desert.

25 Fog in the Namib occurs most frequently near the coast and decreases towards the mountains of the Great Escarpment that separates the Southern Africa inland plateau from the coastal plains. Maximum fog precipitation occurs within a belt at 20–60 km inland from the coast at around 400–500 m a.s.l. (Lancaster et al., 1984; Seely and Henschel, 1998). Directly at the coast and peaking in austral summer (Sep to Mar), advective fog is connected to the southwesterly sea breeze in the afternoon (Seely and Henschel, 1998). Further inland, fog events are described as advected marine stratus clouds coming in 30 touch with the gently rising land ('high fog', Seely and Henschel (1998) (Fig. 1). They are generally associated with north to northeasterly winds at the surface (Seely and Henschel, 1998; Spirig et al., 2019) and feature distinct seasonal characteristics (Lancaster et al., 1984; Seely and Henschel, 1998; Spirig, 2022). In the austral autumn, particularly in April, May, and June (AMJ), the inversion base is very low, and the marine stratus has a low cloud base height of  $\leq 200$  m a.s.l. (Andersen et al., 2019; Yakubu et al., 2025) and is often limited to a coastal strip of  $\approx 25$  km (here called 'fog' from the perspective of a 35 coastal station). During austral summer, and peaking in September, October, and November (SON), the inversion is elevated, the marine boundary layer (MBL) is thicker and the stratus base is higher (here called 'low cloud' from the perspective of a coastal station), with cloud-base heights of 300–500 m a.s.l. and touching the ground only further inland (Andersen et al., 2019; Malik et al., 2025; Yakubu et al., 2025).

40 The marine stratus clouds offshore the Namibian coast (Fig. 1c) form within a shallow MBL over low sea surface temperatures (SSTs), and under a capping temperature inversion related to large-scale subsidence induced by the South Atlantic High (AH) (Andersen et al., 2020). The AH produces coast-parallel winds in the marine boundary layer from the south-southeast (SSE). This SSE wind stabilizes the atmosphere and the offshore low cloud deck, as it advects cool air into the stratus/stratocumulus region, and is strongest in October due to the latitudinal position of the AH (Fig. 1b) and the land-sea thermal contrast during that season (Zuidema et al., 2009). Mostly in austral winter (June to July), a second high pressure develops over the 45 southern African continent (already visible in the AMJ median in Fig. 1a) and the warm and dry air from the continental interior overrides the development of the coastal MBL, possibly reinforcing the shallow inversion that caps the moist and cold marine boundary layer (Preston-Whyte and Tyson, 1988; Tyson et al., 1996; Zuidema et al., 2009; Andersen et al., 2020). Variability at the described synoptic scales influences marine stratocumulus clouds (De Szoek et al., 2016; Fuchs et al., 2017, 2018), and modulates the regional scale thermotopographic circulation (Tyson and Seely, 1980) that determines the inland advection and 50 lifetime of marine fog and low clouds (FLCs) (Seely and Henschel, 1998; Andersen et al., 2020; Mass et al., 2025) and thus regional fog occurrence.

The regional circulation in the Namib Desert is driven by temperature differences between the ocean, flat plain, and mountain surfaces (Weischet and Endlicher, 2000). A moderate SW sea breeze of  $5–10\text{ m s}^{-1}$  (Seely and Henschel, 1998) begins in the late morning at the coast due to stronger heating of the land surface and brings moist cool air from the ocean. Especially in

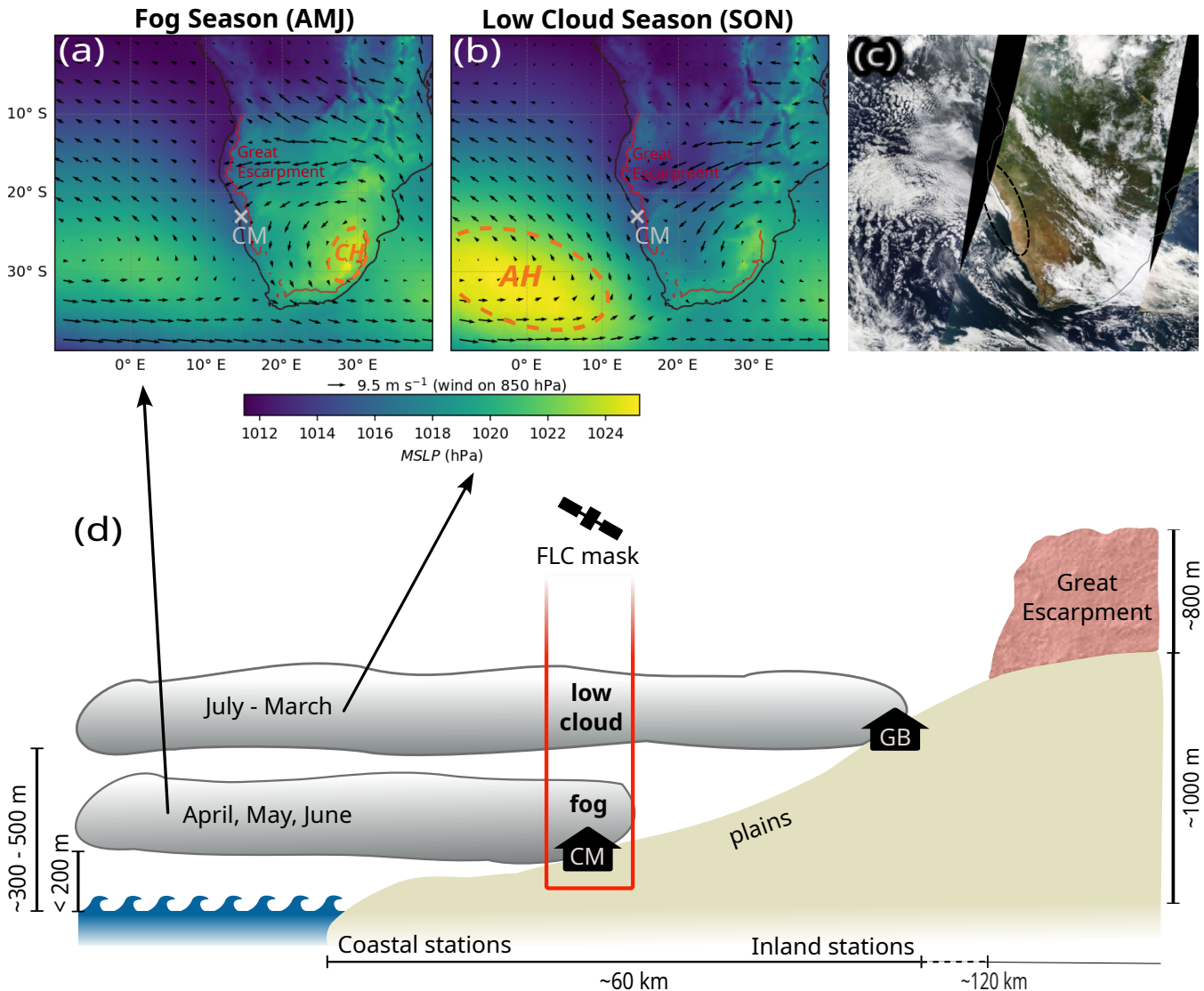


**Figure 1.** Known seasonal patterns of Namib high fog on different altitudes (= fog and low cloud) and study setup. Median composites of the fog (a) and the low cloud (b) peak season featuring synoptic patterns, MODIS Terra snapshot of 23. April 2025 taken from EOSDIS Worldview, showing advected marine stratus forming high fog in the Namib (c) and overview of terms, locations, and data sources, adapted from Andersen et al. (2019) (d). AMJ = April-May-June, CM = Coastal Met station, CH = continental high pressure, SON = September-October-November, AH = Atlantic high pressure, FLC = fog and low clouds, GB = Gobabeb station. The location of the Great Escarpment in (a) and (b) is approximated by the 1000m elevation contour.

55 austral summer (December, January, February, DJF), a second temperature gradient develops between the hot mountains of the Great Escarpment and the cooler flat plain and causes a strong northwesterly wind of  $10 - 15 \text{ m s}^{-1}$  to start blowing in the late afternoon (Seely and Henschel, 1998). This plain-mountain wind keeps blowing until around midnight and overlasts the



sea breeze, which cedes at dusk. With the afternoon NW wind, fog or low stratus clouds from the ocean creep onto the land (Andersen et al., 2019) and hinder nocturnal radiative cooling. The bare inland and mountain regions cool down faster, thus 60 reversing the temperature gradient of the day, especially in austral winter (June, July, August, JJA). The resulting cool katabatic SE mountain-plain wind blows with  $5 - 10 \text{ m s}^{-1}$  from the Escarpment down to the sea, increasing until dawn. In winter, strong, warm, and dry bergwinds can occur, which blow from the Escarpment (Seely and Henschel, 1998) and increase temperatures on the ground by up to 10 K (Weischet and Endlicher, 2000). In particular, the plain-mountain and mountain-plain winds have been connected to the occurrence of low clouds (Seely and Henschel, 1998).

65 From the satellite perspective, both fog near the coast and further inland, with their complementary seasonality, are observed as advected marine low stratiform clouds (Olivier, 1995; Cermak, 2012; Andersen et al., 2019; Spirig et al., 2019) (Fig. 1d) occurring at varying altitudes. However, the physical mechanisms that determine the altitude of the advected stratus and, therefore, the fog occurrence spatial patterns, are not understood yet. While satellite imagers can easily observe the spatial extent of fog and low stratus clouds (Fig. 1c), they cannot retrieve cloud-base height to distinguish between the two with high 70 accuracy, neither by microphysical (Cermak and Bendix, 2011) nor by machine learning techniques (Egli et al., 2018). Space-born lidars yield much higher accuracy (Cermak, 2018; Qiao and Wang, 2022), but the spatial and temporal coverage of the scenes is sparse. Hence, no spatially coherent fog occurrence data exists to date.

Given the advective nature and the contrasting seasonality between fog and low clouds, it seems plausible that synoptic-scale 75 variability contributes to the elevation of the stratus and thus to the occurrence of one or the other. However, it is not yet clear which meteorological aspects of the variability are mechanistically related to fog vs. low-cloud occurrence. One reason for this knowledge gap is the current inability to distinguish fog and low clouds directly from satellite imagery. More specifically, the large-scale high-pressure systems in the South Atlantic and over continental southern Africa have been suggested to drive the spatial extent of fog in the Namib (Lancaster et al., 1984) and are linked to FLCs in the different seasons (Andersen et al., 2020). Easterly winds occurring primarily during the fog season (Fig. 1a) have been related to the seasonal thinning of the 80 MBL (Veloso et al., 2024) and were also found in a simulation of a fog event in September (Hacker, 2024), yet a systematic explanation of the large intraseasonal variability of the MBL height (Veloso et al., 2024) is still missing.

This study aims (i) to characterize the meteorological situations during the two fog variants and (ii) to investigate the extent to which the identified drivers can be used to classify the satellite-based FLC product into fog and low clouds. We combine fog 85 records of a representative near-coastal station with satellite information on FLCs to create a dataset encompassing both fog and low-cloud events from the perspective of a coastal site (CM in Fig. 1d). We then use reanalysis data and a statistical model to address the following specific hypotheses:

1. Seasonal and intraseasonal variability of the two high-pressure systems influences the regional thermotopographic circulation and the altitude of the capping inversion and thus the occurrence of fog vs. low clouds.
2. Information on meteorological drivers can be exploited to separate fog from low clouds in a satellite-based FLC product.



90 **2 Data**

Three main data sources contribute to this study to give a complete analysis.

1. Satellite data from the Spinning Enhanced Visible and Infrared Imager (SEVIRI)
2. The ERA5 dataset, a reanalysis of global hourly meteorological variables
3. In situ measurements from the 2014 established FogNet, combined with in situ measurements from the NaFoLiCA campaign in Sep/Oct 2017

The satellite-based FLC product is a mask of low-cloud presence, derived from infrared bands of the geostationary satellite SEVIRI, and is described in Andersen and Cermak (2018). FLCs are one single category and are detected with a probability of 94 % and a false-alarm rate of 12 % in a  $3\text{ km} \times 3\text{ km}$  pixel and with a temporal resolution of 15 min (Andersen and Cermak, 2018). The algorithm excludes high ice clouds with spectral thresholds and then identifies FLC by comparing to monthly and annual composites of cloud-free conditions. A further context-plausibility check is applied via an iterative counting of surrounding FLC pixels (Andersen and Cermak, 2018). The product is available for the years 2004 to 2020.

The ECMWF Reanalysis Version 5 (ERA5) is a global coverage reanalysis product with hourly meteorological variables (mean variables correspond to the temporal mean of the foregoing hour) and is used to characterize the large-scale conditions during fog and low-cloud events. ERA5 spans from 1940 to the present and has a horizontal resolution of  $0.25^\circ$  and a vertical resolution 25–50 hPa (Hersbach et al., 2020). It is produced by assimilating multiple observational data sets like station data, radiosondes, and satellite imagery into a numerical model. The variables used in this study are mean sea level pressure (*MSLP*), geopotential (*Z*), mean surface latent heat flux (*LHF*), mean surface sensible heat flux (*SHF*), temperature (*T*), specific humidity (*Q*), relative humidity (*RH*), boundary layer height (*BLH*), wind components (*U*, *V*, *W*), sea surface temperature (*SST*) and temperature at 2 m (*T2M*).

In situ measurements serve as ground truth and have a higher temporal resolution than the first two data sources. We here employ FogNet data from two stations, namely Coastal Met (CM) and Gobabeb (GB). Both measure at 1 min resolution the standard meteorological variables (*RH*, *T*, and wind; see also Spirig (2022)) and additionally fog water input (fog precipitation from here on) with Juvik type fog collectors (Juvik and Nullet, 1995) at 0.002 mm resolution. The relative humidity is measured by a Campbell Scientific CS215 sensor (CampbellScientific, 2013) and is used to check the plausibility of fog occurrence, i.e., relative humidity above 90 %. The measurements of FogNet are available from August 2014 onward, but we will exclusively use data from August 2014 - December 2020, as this aligns with the availability of the FLC product.

GB is located in the inland zone where fog events generally are associated with northwesterly or northerly winds and occur between September and March (Lancaster et al., 1984). CM, on the other hand, is located just 17 km from the sea, at the border of the high fog belt (20–120 km inland, Seely and Henschel (1998)). It thus serves to first identify and then distinguish near-coastal and inland high fog events with the intent to combine them with the FLC product. Based on the predominant northerly winds during fog events at CM (Lancaster et al., 1984; Spirig et al., 2019; Spirig, 2022) and known advection patterns from satellite analyses (?), fog events in CM are expected to be stratus clouds with low cloud base altitude, touching the land at the



station elevation of 94 m a.s.l. Stratus clouds with a higher base altitude may pass CM overhead as a cloud and result in fog further inland. Thus, FLCs derived from the SEVIRI may appear as fog or cloud at CM depending on the altitude of the stratus.

125 We furthermore use data from the Namib Fog Life Cycle Analysis field campaign (NaFoLiCA, Spirig et al. (2019)) that took place in Sep/Oct 2017 in both CM and GB. During this period, two SODARs (sonic detection and ranging MFAS from Scintec) measured wind direction and speed, as well as the three wind components  $U$ ,  $V$ , and  $W$  up to 900 m above ground level at CM and GB in 30 min intervals at 15 m vertical resolution based on the return strength (SNR, signal-to-noise ratio) of an acoustic signal. Furthermore, a ceilometer (CL31 from Vaisala) was installed at CM, complementing the existing installation of another 130 ceilometer (CS135 from Campbell Scientific) at GB. These provide backscatter profiles and cloud base height up to 7 km and 10 km, respectively, at a 1 min resolution (see Malik et al. (2025) for detailed instrument description).

### 3 Methods

To create median composites for the two event types, the dates of fog and low-cloud events were derived by combining station and satellite data and were then used to extract data from the reanalysis.

135 In the first step, the satellite FLC product was used to identify days with FLC presence by selecting days on which FLC is detected in the majority of satellite scenes (min. 5 out of 9) over CM between 4 and 6 UTC, the time of maximum FLC occurrence at CM (Andersen and Cermak (2018)). These FLC days are then divided into fog and low-cloud days using in situ fog precipitation measurements. Fog days were defined as FLC days where any fog precipitation at CM was measured between 4 and 6 UTC (338 days) and enriched by fog events that were not detected by the FLC product (e.g., due to higher-level clouds 140 above, 411 days). Low-cloud days are therefore all FLC days without any fog precipitation in the time window. In total, the data covers a common time span of in situ and FLC data from Jul 2014 to Dec 2020, containing 749 fog and 623 low-cloud days. Consistency checks with in situ relative humidity showed that 97 % of fog events exceed 95 % relative humidity.

#### 3.1 Composite analysis and case study

145 ERA5 composites at 5 UTC were computed by calculating the median pixel value of fog or low-cloud events, respectively, over southern Africa and adjacent parts of the Atlantic Ocean (median composites). Difference maps were created by subtracting the fog from the low-cloud composite. As fog and low clouds at CM feature a contrasting seasonality, the resulting meteorological composites can be expected to have a strong signature of the peak seasons. The composites can therefore not be directly interpreted as being mechanistically linked to fog vs. low clouds. Hence, regions are identified where the composite differences have the same sign in all 4 seasons DJF - MAM - JJA - SON to facilitate interpretation. The heatflux composites 150 were computed additionally at 3 UTC, which is before sunrise in all seasons, to check for radiation influence, and showed no relevant differences to 5 UTC. To examine the specific interplay of the identified general drivers, the fog event of the night of 22/23 Sep 2017 was analysed in more detail and supplemented with the additional ceilometer and SODAR data from the NaFoLiCA campaign. Anomalies from typical September conditions were calculated in units of the standard deviation from hourly mean values of all September events (including clear days).



**Table 1.** Features used in the logistic regression to classify fog and low-cloud days over CM, Namibia. Calculated from ERA5 data at 5 UTC.

feature	description	calculation
$P_{diff}$	Regional mountain-plain pressure gradient as a proxy for the thermotopographic circulation	$MSLP$ coast ( $14.5^{\circ}$ E, $23^{\circ}$ S) - $MSLP$ inland ( $16^{\circ}$ E, $23^{\circ}$ S)
$CH$	Strength of the Continental High (CH)	Median $MSLP$ in the region of consistent differences between fog and low-cloud days, over the southern African continent
$AH$	Strength of the AH	Median $MSLP$ in the region of consistent differences between fog and low-cloud days, over the southern Atlantic Ocean .

155 **3.2 Statistical classification**

A simple logistic regression (Cox, 1958) is used to classify FLC-covered days at CM into fog and low-cloud days using ERA5 data of large-scale features associated with fog vs. low-cloud appearance. The logistic regression resembles a linear regression but uses a sigmoid function that is fitted by maximum likelihood estimation to predict class probabilities (Hosmer Jr et al., 2013). We use the default settings of the Python library scikit-learn (Pedregosa et al., 2011) but without L2-regularisation. The 160 L2-regularisation reduces overfitting in the case of many input variables (Tibshirani, 1996), which does not apply to our study since we only use three variables.

To estimate the model's skill and transferability, we use cross-validation. Because the data is a non-continuous time series (only FLC-covered days), a custom cross-validation algorithm is implemented to achieve 1) minimum temporal correlation between training and test set, and 2) representation of all seasons in the test set. For that purpose, all events within a window of 165 365 consecutive days are used as a test set, and the remaining FLC days are used for training, discarding the 7 days before and after the test window. During the iteration process, the window is moved over the time series in 3-month steps. This results in 23 cross-validation iterations (6 non-overlapping).

As suitable input variables for the logistic regression, the observed patterns from the composite analysis were captured in a range of single-value variables and refined to three meaningful features (Table 1). The features were standardized separately in 170 each iteration of the cross-validation using a pipeline to mitigate the effects of different value ranges.

The performance of the logistic regression is compared to a climatological baseline. Instead of using model predictions, the cross-validation procedure is performed using random draws from the monthly probabilities of fog/low-cloud occurrence. Full years serve as folds. To ensure reliable performance estimates, the random draw predictions for each excluded test year are repeated 1,000 times and averaged.



175 The logistic regression adjusts a weighting coefficient for each feature during training. These coefficients can, in case of reasonable model predictions, be interpreted as feature importance ranking the features on their information content concerning the target variable.

## 4 Results and discussion

### 4.1 Large-scale meteorological differences between fog and low clouds

180 Fog and low clouds at CM show a pronounced alternating seasonality (Fig. 2). The months April-May-June (AMJ, indicated by the red bars at the top of the figure) capture the peak fog season, while the months September-October-November (SON, blue bars) are dominated by low clouds. This seasonality agrees roughly with Veloso et al. (2024), who find a deeper MBL during austral summer and a thinner MBL during the fog peak season in early winter. The peak occurrence time can vary considerably between years, as 2017 shows a late fog peak in August and September compared to the expected peak time in May and June  
185 (e.g., in 2018). The usual low-cloud peak is missing in November / December 2019, followed by irregular fog peaks during 2020, which makes these two years show unusual FLC occurrence.

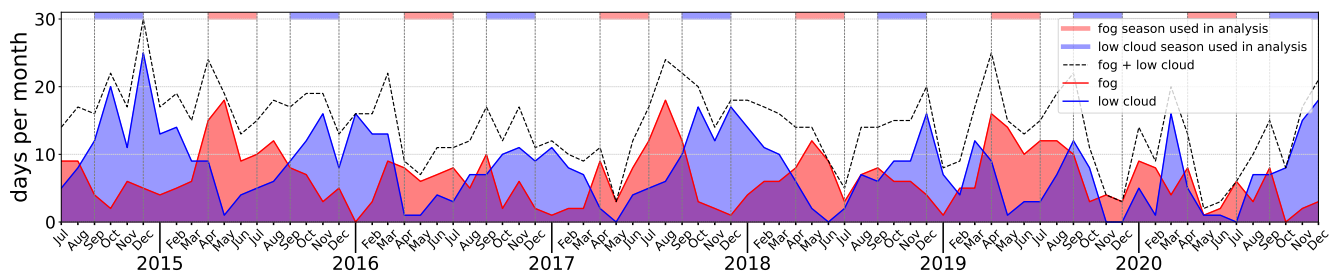


**Figure 2.** Time series of fog and low-cloud events during 4-6 UTC at CM, according to combined SEVIRI-based low-cloud data and in situ fog precipitation. Bars at the top indicate the peak seasons at CM of fog (red, April-May-June) and low clouds (blue, September-October-November).

190 To examine the key drivers beyond peak season characteristics, we compare fog events during the whole year to low-cloud events during the whole year using median composites of meteorological variables (Fig. 3). A pattern of dipolar pressure differences appears in the composites of the fog vs. low-cloud events (Fig. 3a-c), resembling the peak season conditions (Fig. 1a, b). The outlined differences are consistent throughout the year (all four mean differences during DJF, MAM, JJA, SON have the same sign, e.g., MSLP is greater in all four seasons) and may thus point to a physical link to stratus altitudes and, thereby, to spatial fog occurrence patterns. In the following, the consistent differences over the ocean are described and discussed first, followed by the consistent differences over the southern African continent.

195 Low-cloud situations show higher pressure (red) and about 27 % stronger anticyclonal winds on the northeastern flank of the AH, at  $\approx 30^{\circ}\text{S}$  (Fig. 3c). In the region of increased surface winds, increased upward latent and sensible heat fluxes are

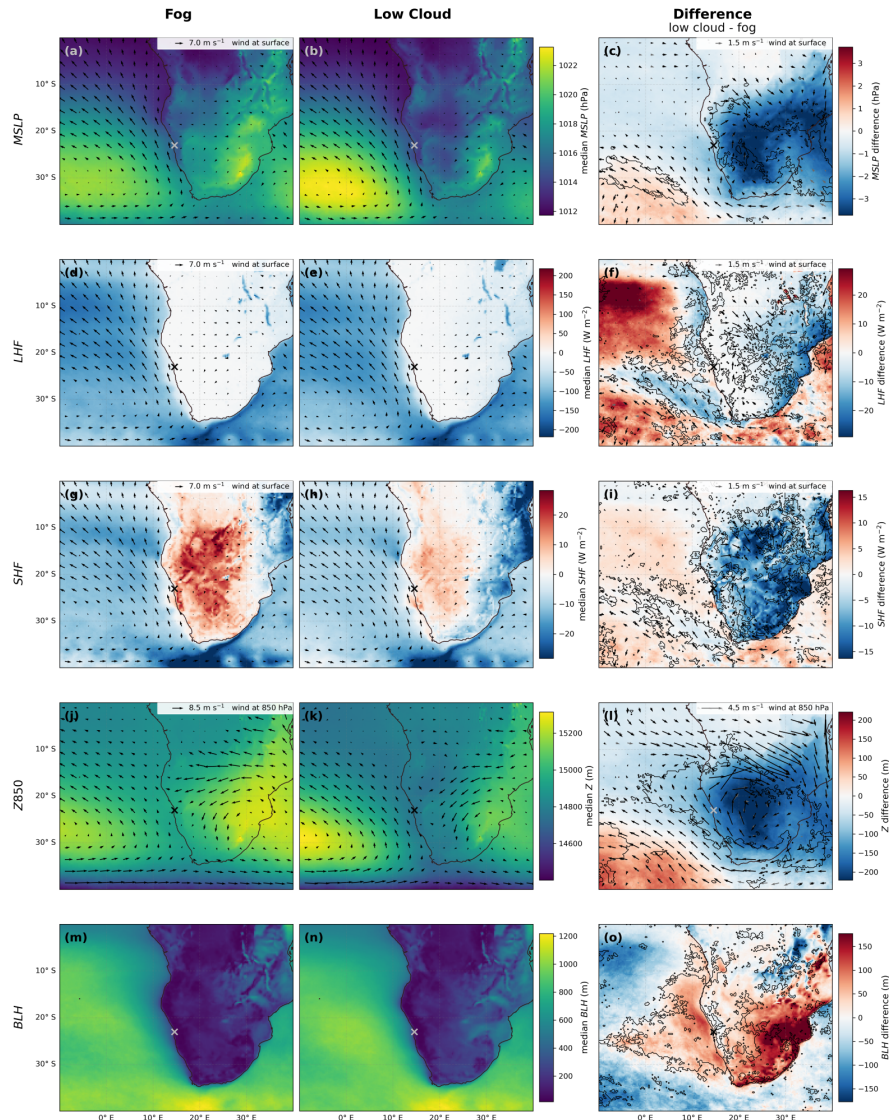


**Figure 3.** Median synoptic situation at 5 UTC during fog (left column) and low-cloud (central column) events at CM (x) and their differences (right column). Regions where the differences are consistent throughout the year (same sign) are highlighted with outlines for the variables a, b, c: mean sea level pressure (MSLP); d, e, f: geopotential height at 850 hPa (Z850); g, h, i: mean surface latent heat flux (LHF); j, k, l: mean surface sensible heat flux (SHF); m, n, o: boundary layer height (BLH). Arrows show  $U$  and  $V$  wind on the corresponding pressure level or at the surface, in black ( $U$  or  $V$  have the same sign differences throughout the year) or grey (none of the two has the same sign differences). Flux direction is negative upward, so the blue (red) difference indicates stronger (weaker) upward fluxes during low-cloud events compared to fog. Data from ERA5. Where the land surface is higher than the given pressure level, values are meaningless.



apparent during low-cloud situations (outlined blue in Fig. 3f, i, as fluxes are negative upward and generally upward over the ocean during both fog and low clouds in Fig. 3d, e, and g, h).

The differences in geopotential at 850 hPa (Fig. 3l) appear similar to the *MSLP* differences (Fig. 3c) with lower values over the continent (blue) and higher values (red) in the AH region in low-cloud situations. However, the region of seasonally 200 consistent lower geopotential extends from the continent over the ocean (Fig. 3l). In this marine region and extending offshore, the MBL is consistently deeper in low-cloud situations (Fig. 3o), particularly near the Namibian coastline northwest of CM, where the median difference in MBL depth is up to 130 m.

We interpret the composites and their differences in terms of processes as follows. The more pronounced AH in low-cloud situations produces the observed stronger coast-parallel southeasterly winds at  $\approx 30^{\circ}\text{S}$ . This causes increased cold-205 air advection from the south, which likely drives the intensified sensible and latent heat fluxes into the MBL in low-cloud situations. Increased upward heat fluxes indicate a stronger contrast between cool air over warm ocean water, leading to unstable conditions, stronger evaporation and heat uptake from the ocean, and have been found to result in a deeper MBL by increasing the buoyancy and the vertical mixing in the MBL (Jury and Walker, 1988; Zheng et al., 2021). Indeed, Andersen et al. (2020) found that specific humidity in MBL air masses is higher on FLC days than on clear days already at least 24h before 210 the FLC event occurs in the Namib. This suggests that the development of the MBL over multiple days critically determines its moisture content, depth, and the resulting stratus altitude.

The AH also drives a coastal jet centered at around  $\approx 20^{\circ}\text{S}$  (Nicholson, 2010), which is weakest in May and June during the fog peak season and most pronounced during the low-cloud peak season. The jet evolves when winds from the AH are deflected into a coast-parallel direction by the elevated terrain, and it advects cold air into the marine stratocumulus region, 215 thereby enhancing stability and cloud formation (Zuidema et al., 2009). While our results do not show local differences in wind speeds at this latitude between fog and low-cloud days, a link to stratus altitude is likely and warrants further attention in the future.

Over the southern African continent, low-cloud situations feature lower *MSLP* (blue), and a less pronounced influence of continental airmasses at the coast. One should note that *MSLP* is likely affected by the elevation of the topography in southern 220 Africa. The difference in the wind patterns is even more pronounced at 850 hPa than at the surface, featuring less continental easterly winds arriving at the coast in low-cloud situations (Fig. 3l).

In both fog and low-cloud situations, the cool and moist coastal MBL is capped by warm and dry air (yellow in Fig. 4a, b, and blue in d, e), forming an inversion that lowers and strengthens towards the continent. The vertical position of this inversion 225 cap is lower during fog situations throughout the seasons (Fig. 4c, f) and along the entire Namibian coast (Fig. 4i), confining the shallow BL. The inversion cap in fog situations is warmer than during low-cloud situations (Fig. 4a, b).

There are also differences in the regional circulation. The zonal circulation pattern over the ocean is shifted vertically by one reanalysis pressure level (25 hPa), with a turnaround from easterly winds near the surface to westerly winds at 850 hPa (fog) vs. 825 hPa (low cloud) where temperatures decrease again (Fig. 4a, b). This vertical shift appears consistently throughout the seasons with free troposphere (FT) winds between 750 and 900 hPa having a consistently weaker eastward component in 230 low-cloud situations, visible by the easterly direction of the residual wind vector in Fig. 4c. The subsidence over the Great

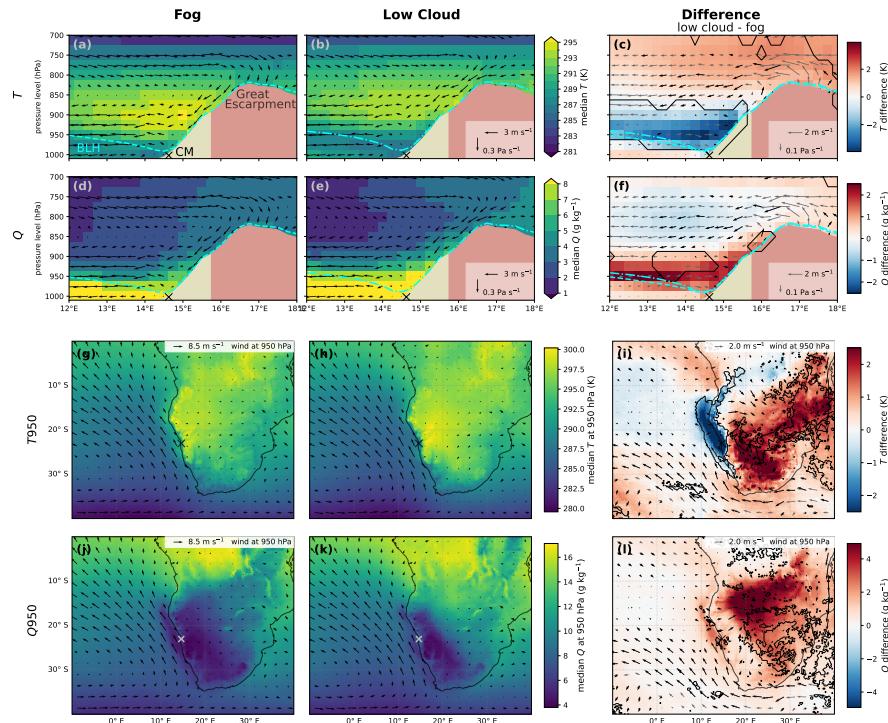


**Figure 4.** ERA5 median vertical structure of the regional atmosphere at 23°S, 5 UTC for a, b, c: temperature ( $T$ ) and d, e, f: specific humidity ( $Q$ ) with u and w wind (arrows) and boundary layer height (BLH). Maps of g, h, i: the 950 hPa level temperature ( $T950$ ) and j, k, l: specific humidity ( $Q950$ ) with u and v wind (arrows). Composites of fog (left) and low-cloud (centre) events at Coastal Met, Namibia (x) and their differences (right). Seasonally consistent differences are highlighted with outlines and black wind arrows.

Escarpment is consistently less pronounced in low-cloud situations and vice versa, more pronounced in fog situations (Fig. 4a-f). In both fog and low-cloud situations, the subsiding air masses follow the topography towards the coast, likely adiabatically heating along the way. In fog situations, this easterly flow is slightly stronger and persists to lower elevations, thus reaching closer to the coast.

235

The described difference patterns likely work together to modulate the altitude of the advected stratus via the following processes. The elevated continental pressure in fog situations prevents substantial convective mixing over the Namib region and thereby facilitates the formation of a temperature gradient between the Great Escarpment and the plains. The resulting intensified easterly mountain-plain wind reaches lower areas closer to the coast, thereby counteracting inland stratus advection. The subsidence and adiabatic heating of the easterly air masses are likely to contribute to the lower inversion and increased



240 temperatures immediately above during fog events. In low-cloud situations, the surface cooling and subsidence over the Great Escarpment are somewhat balanced by weak easterly advection of warm air from within the continent.

Lower continental pressures have already been related to inland-reaching FLC occurrence (Andersen et al., 2020) and longer persistence of FLC events (Mass et al., 2025). Warm easterly continental winds are associated with lower cloud base height of Namibian FLCs during events with limited inland extent in simulations (Hacker, 2024). These simulated low-lying fog events 245 featured warmer capping air and a stronger inversion, in line with the satellite and ERA5 data. Hacker (2024) suggests that a merging of the continental NE wind with SE trade winds may result in a strengthening of the capping inversion. Easterly continental winds have also been found to cause a shallower MBL offshore the central Namib during the fog season March– 250 August, with decreased FLC cover, especially in the region north of CM (Veloso et al., 2024), where we observe the greatest BLH differences between fog and low-cloud situations. Following up on our process understanding, the wind descending from the Great Escarpment and the associated adiabatic heating effect are at some point likely to overwhelm any local coastal effect and decimate any chance of FLC.

From the composite analysis, we summarize the following seasonally consistent large-scale characteristics of low clouds compared to fog (and vice versa): 1) A stronger AH produces stronger MBL winds, cold air advection, and enhanced sensible and latent heat fluxes upstream of the study region, in combination leading to a deeper marine BLH during low cloud cases. 2) 255 Lower continental pressures and less subsidence over the Great Escarpment may inhibit the full development of the subsiding mountain-plain winds, thereby allowing for the higher inversion, in particular close to the coast.

#### 4.2 Case study: Fog outside the peak season

In the following, an anomalous fog event that occurred during the low-cloud season is used to assess how the identified 260 meteorological differences may contribute to day-to-day variability in stratus altitude and out-of-season occurrence of fog at CM. The event occurred during the NaFoLiCA campaign and is partially documented in Spirig et al. (2019).

During the night of 22/23 Sep 2017, a stratus is advected over CM with a cloudbase height consistently below 100 m a.g.l., appearing as fog from about 23:00 to 06 : 30 UTC at CM with almost no lowering and lifting (Fig. 5a). During the nights before and after, a low stratus is advected at 300–500 m a.g.l. that either stays lifted as a low cloud (leading to fog further inland, 20/21 Sep) or lowers towards the surface, leading to fog precipitation at CM, and then strongly lifts and dissipates after 265 sunrise (19/20, 21/22, 23/24 Sep). The sudden appearance of a very low cloud base height during the case study possibly points to a generally low stratus layer and thus to a shallow MBL. A limited stratus extent is apparent on the available MODIS Terra image at 9 UTC (Fig. 5b), showing a narrow 20–30 km wide coast-parallel cloud strip that has, at that time, already been shifted back towards the ocean.

The synoptic situation during this specific fog event (Fig. 6b) shows characteristics that were identified as typical for fog 270 events and that differ from the climatological September conditions that typically produce the higher-altitude low clouds at CM during this time of year (and the days before and after the event, Fig. 6a, c). The first characteristic is the higher pressure over the southern African continent (Great Escarpment and Kalahari) compared to the nights before and after. It is here caused by the formation of a ridging high-pressure circulation pattern over the subcontinent following the passage of a mid-latitude

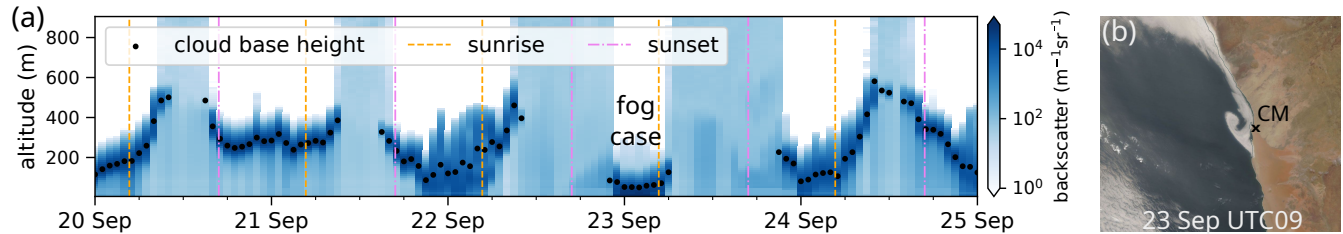


**Figure 5.** The fog event 23rd Sep 2017 from the station and the satellite perspective. a) Hourly mean backscatter and cloud base height 20th Sep 2017 to 25th Sep 2017 at CM, Namibia, data from a CL31 ceilometer; b) MODIS image at about 9 UTC 23rd Sep 2017, featuring remaining coastal stratus clouds of the fog event in the night. Image taken from EOSDIS Worldview.

275 cyclone which impacted the continent at about 30°S. The second characteristic is the wind at 850 hPa coming from the AH and passing over the continent to arrive at CM from SE, there contrasting the calm local conditions during the nights before and after. As a third characteristic, the coast-parallel southeasterly winds are weakly developed because of the position of the AH, also one day before the event.

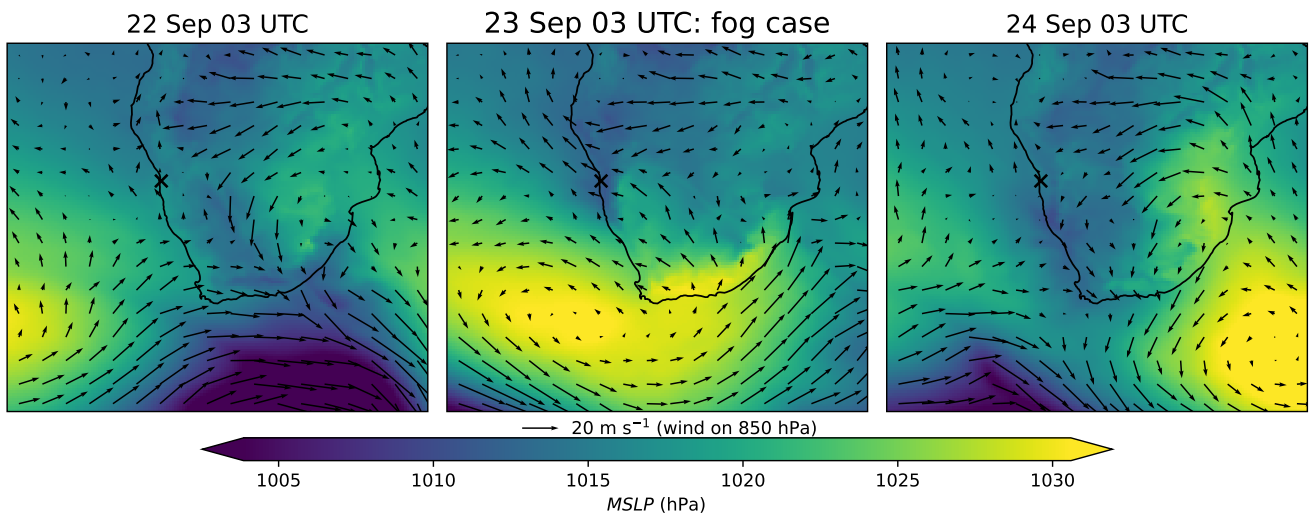


**Figure 6.** Evolution of the synoptic situation one day before the fog night 2017-09-22/23 until one day after (mean sea level pressure (MSLP) and wind on 850 hPa). The fog was measured in Coastal Met, Namibia (x).

280 The vertical structure of the regional atmosphere is shown in a zonal cross-section along the station latitude 23°S (Fig. 7b, e, h). The air masses coming from the continental interior turn into a strong downward wind of up to about 2 Pa/s vertical and 20 m/s easterly wind speed, blowing over the Great Escarpment and down to the top of the coastal boundary layer. Such strong winds co-occurring with ridging highs have been described as bergwinds (Lancaster et al., 1984; Tlhalerwa et al., 2005; Ndarana et al., 2018) and are often strong enough to disrupt the stable surface layer, typically leading to the dissipation of



285 low stratus clouds. The wind may have caused the clear sky over most of the Namib and the ocean without dissipating the small coastal FLC strip. It may have also been deflected by the wind shear with the northerly coast-parallel surface wind that was measured at CM and that likely advected the stratus from the low-cloud deck over the ocean about 350 km north of CM (Fig. 5b). This particular fog event can be interpreted as an intensified version of the typical fog situation shown in the composites. The described effects of the bergwind are similar to the effects of the easterly flow in the composites that were ascribed to the mountain-plain wind.

290 The comparably shallow coastal boundary layer is capped by a strengthened inversion with temperatures up to 301.8 K (28.7°C) (Fig. 7a-c), likely caused by adiabatic heating of the subsiding air masses. The wind seems not to penetrate the cool and moist boundary layer containing the stratus. Rather, the wind is deflected offshore at the top of the BL, at the same time likely pushing it down and towards the coast (Fig. 7b, e, h). The continental easterly wind thereby seems to limit the inland extension of the MBL and a further inland advection of the stratus. The actual advection of the stratus is not visible in these 295 curtain plots because it happens with northerly winds (FLC extension from northerly FLC deck in Fig. 5b, nocturnal northerly wind (blue) during nights in CM in Fig. 8b). The inversion strengthening and subsidence are more extreme in this case than in the median composites of fog, pointing to a strong synoptic forcing.

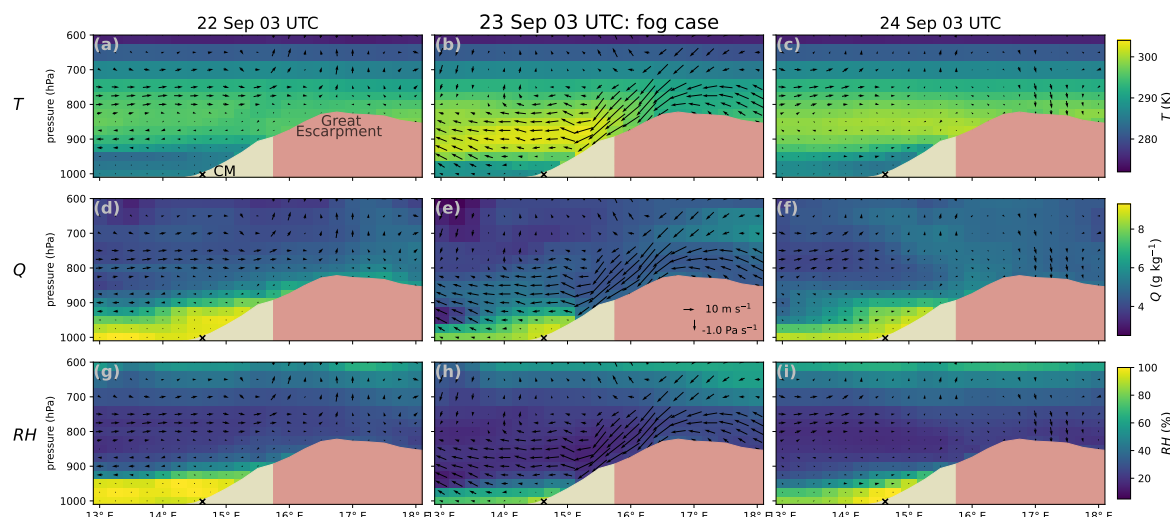


**Figure 7.** Regional circulation during the fog event at CM, Namibia (x), at 3 UTC, compared to the night before and after in latitudinal curtain plots at 23°S.

The meteorological characteristics related to fog occurrence are extraordinarily pronounced during this specific event compared to mean September conditions (Fig. 8a), pointing to its exceptional nature. The anomalies are even more pronounced inland (GB) than at the coast (CM), highlighting that the mechanisms leading to fog near the coast are of regional to synop-



300 tic scale. Anomally increased temperatures ( $1-2\sigma$ ) at the altitude of the inversion ( $T950$ ) together with extraordinary inland  
 easterly-downward wind ( $-4\sigma$ ) around 900 hPa ( $U900$ ,  $W875$ ) indicate the warm-air advection from the continent and adia-  
 batic heating. Ground-based wind measurements (SODAR) confirm the easterly wind component and show that it appears only  
 305 from about 450 m a.g.l. upwards as a surface wind at GB but about 500 m above ground at CM, there due to limited range only  
 observed after 10 UTC (Fig. 8b). The anomaly in the regional pressure difference ( $-1\sigma$ ) developing over the night (Fig. A1)  
 that approximates the thermotopographic winds ( $P_{diff}$ ) is less pronounced than in the occurring winds, indicating a strong  
 310 synoptic forcing on the local winds in the free troposphere.

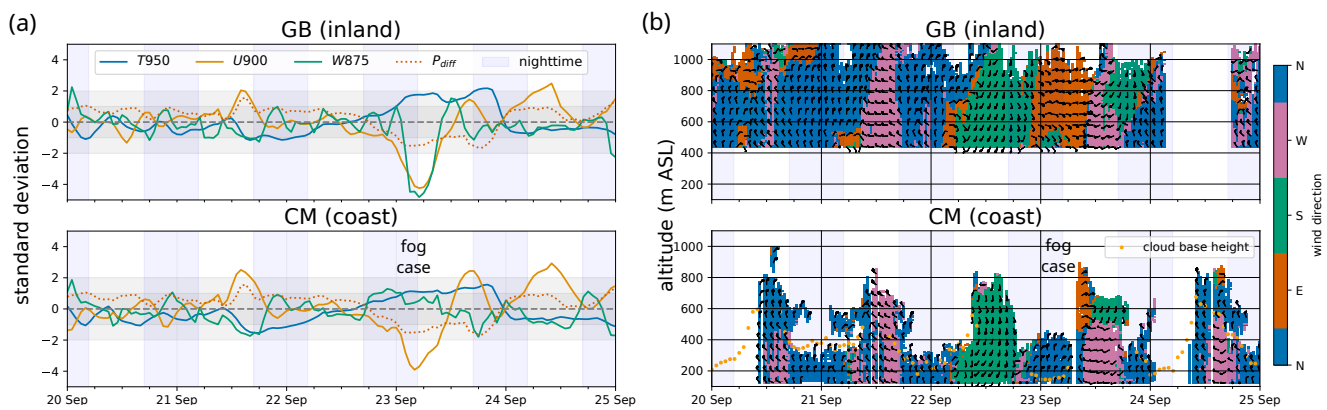


**Figure 8.** Meteorological conditions in Coastal Met (CM) and Gobabeb (GB) during the week of the fog event, 23 Sep 2017 at CM. a) Anomalies to the typical September day (hourly data 2014–2020) of temperature at 950 hPa ( $T950$ ), the eastward wind component at 900 hPa ( $U900$ ), upward wind component at 875 hPa ( $W875$ ), and a regional mountain-plain pressure gradient ( $P_{diff}$ , not site-specific) from ERA5 data. b) In situ wind direction (colours) and vertical component (bars) from SODAR.

310 The case study highlights that mechanisms at the regional to synoptic scale control the local boundary layer and the char-  
 acteristics of this fog situation. In this exceptional fog event, the fog-promoting processes over the southern continent that were  
 identified in the composite analysis are exceptionally pronounced. The case thus supports the concept of a stratus cloud that  
 is limited in vertical and inland extent by a low coastal inversion induced by easterly winds from the continent, initiated by  
 synoptic-scale pressure patterns. We also conclude that fog precipitation at CM can be connected to two different high fog sit-  
 uations: 1. a very low cloud base touching the ground when it is advected to CM (typical for AMJ, but can also be synoptically  
 forced out of season), or 2. stratus base lowering after the advection of the stratus has already taken place (as shown by the  
 315 ceilometer in the fog nights before and after the case night).

#### 4.3 Classification of fog and low clouds

A logistic regression model was trained to classify FLC days into fog or low-cloud days with three features capturing the CH, AH, and regional thermotopographic circulation (described in Tab. 1). With only these three meteorological features, the

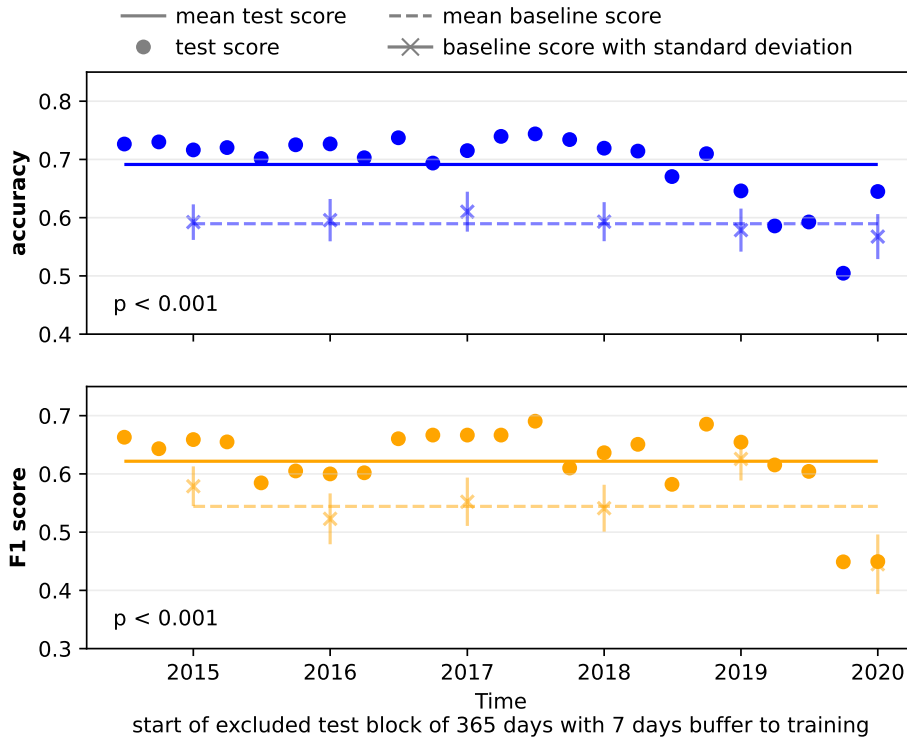


**Figure 9.** Logistic regression with three features capturing the CH, AH, and thermotopographic circulation, compared to a climatological baseline.

model achieves a cross-validated 69.1 % accuracy and thus excels the mean baseline by 10.1 % (f1-score increase of 7.7 % from 54.5 % baseline to 62.2 %, Fig. 9). The mean baseline accuracies for the test years 2015–2020 are 0.594, 0.594, 0.613, 320 0.594, 0.578, and 0.567, respectively, illustrating that guessing fog/low cloud from seasonality is better than a random pick (accuracy = 0.5 to distinguish the event types for a given FLC event). The applied split method in the cross-validation allows for comparing the performance on different test sets of 365 days (Fig. 9). The events in 2019 and 2020 are predicted with a lower accuracy, which may be related to the disrupted and unusual occurrence patterns of fog and low clouds during the two 325 years (Fig. 2). Indeed, a Benguela Niño occurred between October 2019 and January 2020 with SST anomalies of more than 2 °C, preceded and accompanied by anomalous latent heat fluxes and winds (Imbol Koungue et al., 2021).

As the model based on meteorological features outperforms the baseline, the features contain information related to the target variable fog or low cloud. Among the three features, the CH feature is ranked most important based on model coefficients, followed by the AH feature and the local pressure difference between mountains and coast ( $P_{diff}$ , see Tab. 1). This suggests a framing role of the synoptics, at the same time highlighting the importance of the regional mountain-plain wind for the 330 elevation of the stratus clouds. The results also highlight the potential to use reanalysis information to separate fog from low clouds in satellite-based FLC products, in particular, when local temperature and humidity profiles are additionally used.



## 5 Conclusions

This study is a first characterisation of meteorological conditions associated with the altitude of high fog in the central Namib that, in turn, determines the locations receiving fog (Fig. 10). Two hypotheses guided this work: that fog (high fog touching the ground) and low-cloud occurrence at CM are connected to variability of the continental and Atlantic high pressure systems and regional thermotopographic winds (H1) and that information on these meteorological characteristics can be used to classify fog/low clouds (H2). A composite analysis and a case study are conducted to test H1, where the composite analysis additionally tests for consistency over the seasons. The main findings of this study are:

- The boundary layer is systematically shallower in fog situations than in low-cloud situations along the entire southwestern African coast, particularly in marine regions close to Walvis Bay. In fog situations, the capping inversion is therefore lower, and the capping air is warmer. The differences in the depth of the marine boundary layer and stratus altitude are related to the variability of the two high-pressure systems in the regions.
- Over the ocean, the South Atlantic Anticyclone is stronger in low-cloud situations than in fog situations, leading to stronger MBL winds and increased cold advection at  $\approx 30^{\circ}\text{S}$  and into the stratus formation region. This probably causes the observed increases in latent and sensible heat fluxes into the MBL in that region, which would deepen the developing MBL by increasing its buoyancy and vertical mixing.
- Over the continent, fog situations at CM are associated with higher pressures over the Great Escarpment and the Kalahari than low-cloud situations. These higher pressures are thought to facilitate the development of the nocturnal subsiding easterly mountain-plain winds, which are observed to be more pronounced during fog situations, possibly pushing down the coastal inversion from above.
- In a case study, an out-of-season fog event that occurred during September 2017 is analyzed in detail. The case is strongly influenced by a ridging high-pressure system that imposes similar but amplified large-scale characteristics of typical fog cases: higher pressures over the south-west African continent and strong subsiding easterly continental air masses that seem to push down and strengthen the inversion, leading to a particularly low-lying stratus and spatially limited fog event on this day. The ridging high leads to a disruption of the regional circulation and is thought to prevent a further inland advection of the low-cloud layer as seen on the days before and after the event.
- A logistic regression was used to classify fog and low clouds based on three meteorological features describing the South Atlantic and continental high-pressure systems and the regional mountain-plain circulation. The logistic regression has a 69 % accuracy and 62 % F1-score, outperforming the climatological baseline by 10 % and 7 %, respectively. This underlines that the two large-scale high-pressure systems, as well as the regional thermotopographic circulation, are relevant controls of the capping inversion and stratus altitude.

The findings of this study highlight the connection between synoptic-scale variability and regional thermotopographic circulations that, in tandem, determine the seasonal patterns and day-to-day variability of the altitude of the capping inversion,

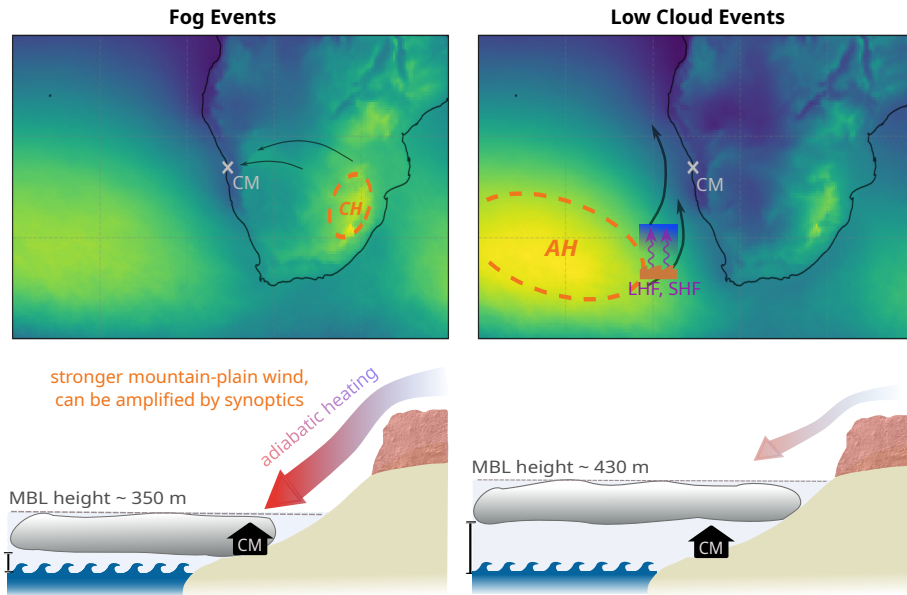


**Figure 10.** Schematic description of synoptic-scale and regional patterns and processes associated with fog events vs. low cloud events in the Namib. The MBL height is an averaged value of a  $1^{\circ}$  wide strip along the coast from  $17.5^{\circ}\text{S}$  to  $31^{\circ}\text{S}$  (about 100 km wide).

the stratus altitude, and subsequent spatial fog occurrence patterns. Future studies should investigate these relationships for  
365 specific synoptic circulation types.

*Code and data availability.* ERA5 data were taken from Copernicus Climate Data Store. The satellite FLC product and code for data processing and analysis are available from the corresponding author upon reasonable request.

## Appendix A: Appendix

*Author contributions.* HA had the initial idea for the study and provided the FLC product. RV and RS provided the in situ station data.  
370 VH acquired the ERA5 datasets and designed, developed the code for, and performed the statistical analysis and classification in exchange with HA and JC. RS provided visualisations of in situ data. BA contributed to heat flux interpretation. SP contributed to the meteorological interpretation. VH wrote the manuscript with contributions by all authors. All co-authors contributed to the overall interpretation of the results and manuscript editing.

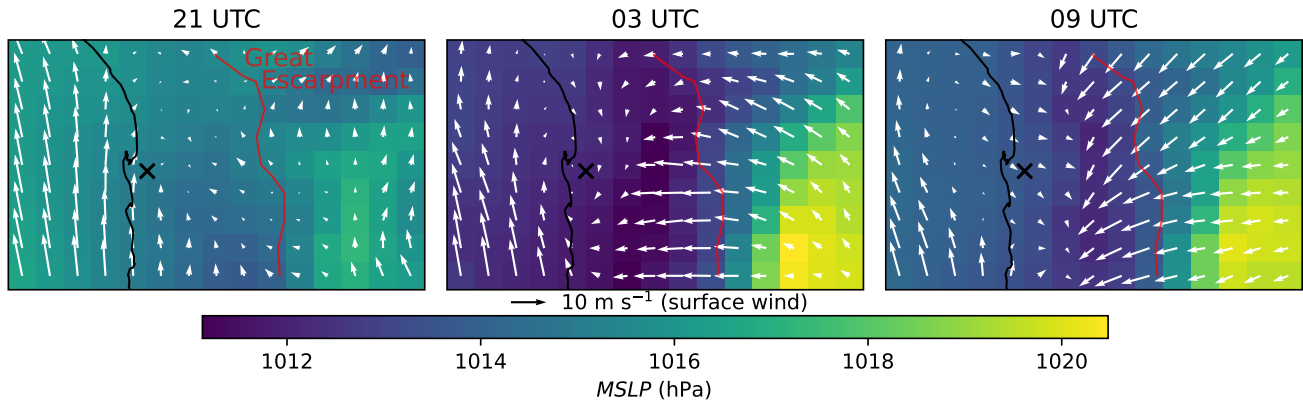


**Figure A1.** Mean sea level pressure ( $MSLP$ ) during the fog night 22./23.09.2017. Quivers denote the surface wind at 10 m. The red line provides an approximate indication of the Great Escarpment (1000 m elevation contour).

*Competing interests.* The authors declare that they have no conflict of interest.

375 *Acknowledgements.* We acknowledge the funding by the Deutsche Forschungsgemeinschaft (DFG, grant no. CE 163/14-1, project no. 505800970) and the Agence Nationale de la Recherche (ANR, grant no. ANR-22-CE92-0051) of the project "Aerosols and fog in southern Africa: processes and impact on biogeochemistry (AeroFog)". The contribution of BA was supported by NOAA cooperative agreement NA22OAR4320151, for the Cooperative Institute for Earth System Research and Data Science (CIESRDS). The statements, findings, conclusions, and recommendations are those of the authors and do not necessarily reflect the views of NOAA or the U.S. Department of Commerce.  
380 The authors would like to thank the Gobabeb Namib Research Institute for access to the station measurements and gratefully acknowledge the Gobabeb maintenance team for their efforts in the field. We acknowledge support by the KIT-Publication Fund of the Karlsruhe Institute of Technology.



## References

Andersen, H. and Cermak, J.: First fully diurnal fog and low cloud satellite detection reveals life cycle in the Namib, *Atmospheric Measurement Techniques*, 11, 5461–5470, 2018.

385 Andersen, H., Cermak, J., Solodovnik, I., Lelli, L., and Vogt, R.: Spatiotemporal dynamics of fog and low clouds in the Namib unveiled with ground-and space-based observations, *Atmospheric Chemistry and Physics*, 19, 4383–4392, 2019.

Andersen, H., Cermak, J., Fuchs, J., Knippertz, P., Gaetani, M., Quinting, J., Sippel, S., and Vogt, R.: Synoptic-scale controls of fog and low-cloud variability in the Namib Desert, *Atmospheric Chemistry and Physics*, 20, 3415–3438, 2020.

390 Burke, A.: Plant endemism in the central Namib Desert, *EVOLUTIONARY ECOLOGY RESEARCH*, 9, 283–297, 2007.

CampbellScientific: CS215 temp and rh probe: user manual, Campbell Scientific, available at: [https://s.campbellsci.com/documents/ca/manuals/cs215\\_man.pdf](https://s.campbellsci.com/documents/ca/manuals/cs215_man.pdf), 2013.

Cermak, J.: Low clouds and fog along the South-Western African coast—Satellite-based retrieval and spatial patterns, *Atmospheric Research*, 116, 15–21, 2012.

395 Cermak, J.: Fog and low cloud frequency and properties from active-sensor satellite data, *Remote Sensing*, 10, 1209, 2018.

Cermak, J. and Bendix, J.: Detecting ground fog from space—a microphysics-based approach, *International Journal of Remote Sensing*, 32, 3345–3371, 2011.

Cox, D. R.: The regression analysis of binary sequences, *Journal of the Royal Statistical Society Series B: Statistical Methodology*, 20, 215–232, 1958.

400 De Szoek, S. P., Verlinden, K. L., Yuter, S. E., and Mechem, D. B.: The time scales of variability of marine low clouds, *Journal of Climate*, 29, 6463–6481, 2016.

Egli, S., Thies, B., and Bendix, J.: A hybrid approach for fog retrieval based on a combination of satellite and ground truth data, *Remote Sensing*, 10, 628, 2018.

405 Fuchs, J., Cermak, J., Andersen, H., Hollmann, R., and Schwarz, K.: On the influence of air mass Origin on low-cloud properties in the Southeast Atlantic, *Journal of Geophysical Research: Atmospheres*, 122, 11–076, 2017.

Fuchs, J., Cermak, J., and Andersen, H.: Building a cloud in the southeast Atlantic: understanding low-cloud controls based on satellite observations with machine learning, *Atmospheric Chemistry and Physics*, 18, 16 537–16 552, 2018.

Gottlieb, T. R., Eckardt, F. D., Venter, Z. S., and Cramer, M. D.: The contribution of fog to water and nutrient supply to *Arthraerua leubnitziae* in the central Namib Desert, Namibia, *Journal of Arid Environments*, 161, 35–46, 410 <https://doi.org/https://doi.org/10.1016/j.jaridenv.2018.11.002>, 2019.

Hacker, M.: Modelling Fog and Low Stratiform Clouds in the Namib Desert with COSMO-FOG, Ph.D. thesis, Universitäts-und Landesbibliothek Bonn, 2024.

Haensler, A., Cermak, J., Hagemann, S., and Jacob, D.: Will the southern African west coast fog be affected by future climate change? Results of an initial fog projection using a regional climate model, *Erdkunde*, 65, 261–275, <https://doi.org/10.3112/erdkunde.2011.03.04.2011>.

Hersbach, H., Bell, B., Berrisford, P., Hirahara, S., Horányi, A., Muñoz-Sabater, J., Nicolas, J., Peubey, C., Radu, R., Schepers, D., et al.: The ERA5 global reanalysis, *Quarterly Journal of the Royal Meteorological Society*, 146, 1999–2049, 2020.

415 Hosmer Jr, D. W., Lemeshow, S., and Sturdivant, R. X.: Applied logistic regression, vol. 398, John Wiley & Sons, 2013.



420 Imbol Koungue, R. A., Brandt, P., Lübbeke, J., Prigent, A., Martins, M. S., and Rodrigues, R. R.: The 2019 Benguela Niño, *Frontiers in Marine Science*, 8, 800 103, 2021.

Jury, M. and Walker, N.: Marine boundary layer modification across the edge of the Agulhas Current, *Journal of Geophysical Research: Oceans*, 93, 647–654, 1988.

Juvik, J. O. and Nullet, D.: Comments on "A proposed standard fog collector for use in high-elevation regions", *Journal of Applied Meteorology (1988-2005)*, 34, 2108–2110, <http://www.jstor.org/stable/26187431>, 1995.

425 Lancaster, J., Lancaster, N., and Seely, M.: Climate of the central Namib Desert, *Madoqua*, 1984, 5–61, 1984.

Loots, S., Ritz, C. M., Schwager, M., Sehic, J., Herklotz, V., Garkava-Gustavsson, L., and Nybom, H. E.: Distribution, habitat profile and genetic variability of Namibian succulent *Lithops ruschiorum*, *Bothalia-African Biodiversity & Conservation*, 49, 1–18, 2019.

Malik, D., Andersen, H., Cermak, J., Vogt, R., and Adler, B.: Cloud Base Height Determines Fog Occurrence Patterns in the Namib Desert and Can Be Estimated from Near-Surface Relative Humidity, *EGUsphere*, pp. 1–24, <https://doi.org/10.5194/egusphere-2025-2645>, 2025.

430 Mass, A., Andersen, H., Cermak, J., Formenti, P., Pauli, E., and Quinting, J.: A satellite-based analysis of semi-direct effects of biomass burning aerosols on fog and low-cloud dissipation in the Namib Desert, *Atmospheric Chemistry and Physics*, 25, 491–510, 2025.

Maúre, G., Pinto, I., Ndebele-Murisa, M., Muthige, M., Lennard, C., Nikulin, G., Dosio, A., and Meque, A.: The southern African climate under 1.5 C and 2 C of global warming as simulated by CORDEX regional climate models, *Environmental Research Letters*, 13, 065 002, 2018.

435 Mupambwa, H. A., Hausiku, M. K., Nciizah, A. D., and Dube, E.: The unique Namib desert-coastal region and its opportunities for climate smart agriculture: A review, *Cogent Food & Agriculture*, 5, 1645 258, 2019.

Ndarana, T., Bopape, M.-J., Waugh, D., and Dyson, L.: The influence of the lower stratosphere on ridging Atlantic Ocean anticyclones over South Africa, *Journal of Climate*, 31, 6175–6187, 2018.

Nicholson, S. E.: A low-level jet along the Benguela coast, an integral part of the Benguela current ecosystem, *Climatic Change*, 99, 613–624, 440 2010.

Olivier, J.: Spatial distribution of fog in the Namib, *Journal of Arid Environments*, 29, 129–138, 1995.

Pedregosa, F., Varoquaux, G., Gramfort, A., Michel, V., Thirion, B., Grisel, O., Blondel, M., Prettenhofer, P., Weiss, R., Dubourg, V., Vanderplas, J., Passos, A., Cournapeau, D., Brucher, M., Perrot, M., and Duchesnay, E.: Scikit-learn: Machine Learning in Python, *Journal of Machine Learning Research*, 12, 2825–2830, 2011.

445 Preston-Whyte, R. and Tyson, P.: The atmosphere and weather of southern Africa, Oxford University Press, 1988.

Qiao, N. and Wang, L.: Satellite observed vegetation dynamics and drivers in the Namib sand sea over the recent 20 years, *Ecohydrology*, 15, e2420, 2022.

Ramond, J.-B., Baxter, J., Maggs-Kölling, G., Martínez-Alvarez, L., Read, D., León-Sobrino, C., van der Walt, A., and Cowan, D.: Microbial ecology of the Namib Desert, in: *Model Ecosystems in Extreme Environments*, pp. 113–143, Elsevier, 2019.

450 Seely, M.: Irregular fog as a water source for desert dune beetles, *Oecologia*, 42, 213–227, 1979.

Seely, M. and Henschel, J. R.: The climatology of Namib fog, in: *Proceedings of the First International Conference on Fog and Fog Collection*, pp. 19–24, Vancouver, 1998.

Shanyengana, E., Henschel, J., Seely, M., and Sanderson, R.: Exploring fog as a supplementary water source in Namibia, *Atmospheric Research*, 64, 251–259, 2002.

455 Spirig, R.: Fog in the Namib - occurrence dynamics properties, Ph.D. thesis, University\_of\_Basel, 2022.



Spirig, R., Vogt, R., Larsen, J. A., Feigenwinter, C., Wicki, A., Franceschi, J., Parlow, E., Adler, B., Kalthoff, N., Cermak, J., et al.: Probing the fog life cycles in the Namib Desert, *Bulletin of the American Meteorological Society*, 100, 2491–2507, 2019.

Tibshirani, R.: Regression shrinkage and selection via the lasso, *Journal of the Royal Statistical Society Series B: Statistical Methodology*, 58, 267–288, 1996.

460 Tlhalerwa, K., Freiman, M., and Piketh, S.: Aerosol deposition off the Southern African West Coast by berg winds, *South African Geographical Journal*, 87, 152–161, 2005.

Tyson, P. and Seely, M.: Local winds over the central Namib, *South African Geographical Journal*, 62, 135–150, 1980.

Tyson, P., Garstang, M., Swap, R., Kallberg, P., and Edwards, M.: An air transport climatology for subtropical southern Africa, *International journal of climatology*, 16, 265–291, 1996.

465 Veloso, J. V., Böhm, C., Schween, J. H., Löhnert, U., and Crewell, S.: A comparative study of the atmospheric water vapor in the Atacama and Namib Desert, *Global and Planetary Change*, 232, 104 320, 2024.

Warren-Rhodes, K. A., McKay, C. P., Boyle, L. N., Wing, M. R., Kiekebusch, E. M., Cowan, D. A., Stomeo, F., Pointing, S. B., Kaseke, K. F., Eckardt, F., et al.: Physical ecology of hypolithic communities in the central Namib Desert: the role of fog, rain, rock habitat, and light, *Journal of Geophysical Research: Biogeosciences*, 118, 1451–1460, 2013.

470 Weathers, K. C., Ponette-González, A. G., and Dawson, T. E.: Medium, vector, and connector: Fog and the maintenance of ecosystems, *Ecosystems*, 23, 217–229, 2020.

Weischet, W. and Endlicher, W.: *Regionale Klimatologie: Teil 2: Die Alte Welt, Europa, Afrika, Asien*, Springer, 2000.

Yakubu, A. T., Klopper, D., Havenga, H., Burger, R., Formenti, P., and Piketh, S. J.: Atmospheric stratification over the Southeast Atlantic Ocean adjacent to the Namibian coast, EGUsphere, <https://doi.org/10.5194/egusphere-2025-1827>, 2025.

475 Zheng, Y., Zhang, H., and Li, Z.: Role of surface latent heat flux in shallow cloud transitions: A mechanism-denial LES study, *Journal of the Atmospheric Sciences*, 78, 2709–2723, 2021.

Zuidema, P., Painemal, D., De Szoke, S., and Fairall, C.: Stratocumulus cloud-top height estimates and their climatic implications, *Journal of Climate*, 22, 4652–4666, 2009.